

# Complementary SAXS and SANS for structural characteristics of a polyurethane elastomer of low hard-segment content

Ya-Sen Sun<sup>a</sup>, U-Ser Jeng<sup>a,\*</sup>, Yu-San Huang<sup>a</sup>, Keng. S. Liang<sup>a</sup>, Tsang-Lang Lin<sup>b</sup>,  
Cheng-Si Tsao<sup>c</sup>

<sup>a</sup>National Synchrotron Radiation Research Center, Hsinchu 30076, Taiwan

<sup>b</sup>Department of Engineering and System Science, National Tsing Hua University, Hsinchu 30043, Taiwan

<sup>c</sup>Nuclear Fuel and Materials Division, Institute of Nuclear Energy Research, Longtan, Taiwan

## Abstract

A polyurethane (PU) elastomer film based on segmented poly(tetramethylene oxide) (PTMO) has been studied using wide-angle X-ray scattering (WAXS), and small-angle X-ray and neutron scattering (SAXS and SANS). The broad WAXS peaks measured for the PU elastomer reveal a low crystallinity of the soft segments PTMO and no crystalline domains for the hard segments, methylene bis(4-isocyanatobenzene) (MDI), at 20 °C. Whereas small-angle scattering indicates the existence of hard-segment-rich aggregates. Using the contrast variation provided by the SANS and SAXS, we have extracted detailed structural information of the aggregates, including the shape, size, and the aggregation numbers.

© 2006 Elsevier B.V. All rights reserved.

PACS: 83.80.Va; 83.85.Hf

Keywords: SNAS; SAXS; Polyurethane; Aggregation

## 1. Introduction

Polyurethane (PU) block copolymers belong to a class of thermoplastic elastomers with microstructures sensitive to chemical compositions of the soft and hard segments employed. [1,2] Due to the coexistence of multi-phases [3] and the slow dynamics of equilibrium phase, [4] the structures and thermal–mechanical properties of PU relate highly to the thermal and mechanical histories of the material. [5] The strong correlation between the microscopic structures and the technologically important macroscopic properties has made polyurethane attractive in academic as well as in commercial research. Numerous studies using various techniques, including DSC, WAXS, [2] SAXS, [1,2,5] FTIR, and NMR have been done. The majority of these studies focused on PU structures of a high hard-segment content above ~30%, where continuous

hard-segment domains can be clearly identified and traced in structural transitions [3,5,6].

On the other hand, PU elastomers of a low hard-segment composition (less than 30%) are believed to have only discontinuous hard-segment domains of a micellar nature [7] in the soft-segment solvent-like matrix, especially when the sequence length of the hard segments is short. [5] In this report, we study the micellar structural characteristics of a segmented PU elastomer, of a low hard-segment content and a short hard-segment sequence length, using the contrast variation provided by SANS and SAXS [8].

## 2. Scattering model and SAXS/SANS contrast variation

Adapting the scattering formulism for aggregates in colloidal solutions, [8] we model the neutron or X-ray small-angle scattering (SAS) intensity for the hard-segment-rich aggregates as

$$I(Q) = I_0 P(Q) S(Q), \quad (1)$$

\*Corresponding author. Tel.: +886 3 5742671; fax: +886 3 5728445.

E-mail address: [usjeng@nsrrc.org.tw](mailto:usjeng@nsrrc.org.tw) (U.-S. Jeng).

where  $P(Q)$  is the normalized form factor with  $P(0) = 1$ , and  $S(Q)$  the structure factor. The wave vector transfer  $Q = 4\pi \sin(\theta/2)/\lambda$  is defined by the scattering angle  $\theta$  and the wavelength  $\lambda$  of either neutrons or photons (X-rays). Whereas the zero-angle scattering

$$I_o = (C - C_o)N(b_h - V_{\text{dry}}\rho_s)^2 \quad (2)$$

depends on the concentration of the hard segment  $C$ , the critical concentration for aggregation  $C_o$ , the aggregation number of hard segment  $N$ , and the scattering contrast between the hard-segment aggregates and the soft-segment matrix of scattering-length-densities  $\rho_h = b_h/V_{\text{dry}}$  and  $\rho_s$ , respectively. Here,  $b_h$  is the scattering length of the hard segment monomer of dry volume  $V_{\text{dry}}$ .

For rod-like aggregates, we use the form factor

$$P(Q) = \int_0^1 \left| \frac{2J_1(v)}{v} \frac{\sin(w)}{w} \right|^2 d\mu \quad (3)$$

which integration takes into account the spatial orientations of right-circular cylinders of radius  $r$  and length  $L$ , with  $v = Qr(1 - \mu^2)^{1/2}$ ,  $w = (1/2)QL\mu$ , and the first order Bessel function  $J_1$ . For hard-segment aggregates with no charge interactions, the structure factor derived from the Percus–Yevick model of hard-sphere interactions may be appropriate [8].

For a two-phase system containing hard segments and soft segments in a segmented PU film,  $I_o$  value in Eq. (1) changes with neutrons and X-rays due to the different scattering lengths  $b_h$  of the material. The scattering profile in Eq. (1) is irrelevant to the radiation quanta used. This contrast variation is equivalent to the hydrogen-deuteration substitution contrast method often used in SANS for polymers. [9] For the case of segmented PU, the scattering length densities estimated for a hard segment monomer of two methylene bis(4-isocyanatobenzene) (MDI) and a soft-segment poly(tetramethylene oxide) (PTMO) are  $\rho_h \sim 13.3 \times 10^{-6} \text{ \AA}^{-2}$  and  $\rho_s \sim 10.2 \times 10^{-6} \text{ \AA}^{-2}$  for X-rays, whereas  $\rho_h \sim 2.84 \times 10^{-6} \text{ \AA}^{-2}$  and  $\rho_s \sim 0.2 \times 10^{-6} \text{ \AA}^{-2}$  for neutrons. Here, we have used monomer volumes 710 and  $3510 \text{ \AA}^3$  for the hard and soft segments, respectively, adapted from a previous study. [10] From the estimated contrast, SAXS intensity for the PU films studied is expected to be slightly higher than neutrons, provided that the hard segments form aggregates. Another aspect revealed from the above estimation is the nearly zero neutron scattering length density for the PTMO matrix, which makes neutrons virtually insensitive to the PTMO matrix as well as the density difference between the amorphous and crystalline domains of PTMO. In contrast, X-rays are much more sensitive to the same density difference due to the high absolute scattering length of the PTMO matrix for X-rays.

### 3. Experimental

Segmented PTMO-based PU elastomer film of a thickness of 0.1 cm was prepared from the reaction of 1,4-butanediol (BD) with diisocyanated prepolymer, as detailed in a previous report. [11] The prepolymers were prepared from poly(tetramethylene oxide) glycol with two equivalents of MDI, at 60 °C under an ambient pressure of  $N_2$ . The number-average molecular weight,  $M_n$ , of PTMO is 2000 g/mol, with a polymerization index (PI) of 2.25. The segmented PU elastomer thus synthesized contains 19.3 wt% hard-segments, with each hard segment monomer consisting of two MDI and one BD extender.

SAXS measurement was performed at a sample temperature of 20 °C on the 8 m SAXS instrument at Tsing-Hua University. The monochromatic beam of  $1.54 \text{ \AA}$  was collimated by three pinholes for a diameter of 1.0 mm. With a sample-to-detector distance of 2.8 m, the data collected by the 2-D detector covered a  $Q$ -range from 0.01 to  $0.2 \text{ \AA}^{-1}$ . The data were corrected for sample transmission, background, and detector sensitivity, and normalized to the scattering cross-section per unit sample volume  $I(Q)$  (the absolute intensity). On the other hand, SANS data were collected at 20 °C on the 8 m SANS instrument at the National Institute of Standards and Technology (NIST). Pinholes of 2.5 cm and 1 cm diameters separated by 4.1 m were used to collimate the incident monochromatic beam of a wavelength dispersion of 25%. With a sample-to-detector distance of 3.6 m and two beam wavelengths of 6 and  $10 \text{ \AA}$ , data in the  $Q$ -range from 0.01 to  $0.17 \text{ \AA}^{-1}$  were collected. The SANS data collected by a two-dimensional detector were normalized to the absolute intensity using the same procedure as that used for the SAXS data.

For SANS, a high incoherent scattering background from the hydrogen atoms in the PU film,  $0.76 \text{ cm}^{-1}$  ( $\lambda = 6 \text{ \AA}$ ), is extrapolated from the high- $Q$  data region of a featureless flat line. The incoherent scattering contribution subtracted from the SANS data is consistent with the value  $0.74 \text{ cm}^{-1}$  calculated according to an empirical formula of Jacrot. [12]

### 4. Results and discussion

Fig. 1 shows the SAXS and SANS data for the segmented PU elastomer film. These two profiles are very similar in a wide  $Q$  range, except the sharp raising peak for SAXS in the  $Q$  region lower than  $0.02 \text{ \AA}^{-1}$ . The result indicates a general two-phase structure for the system [13] consisting of hard-segment-rich aggregates in the PTMO matrix. As to the low- $Q$  sharp peak observed in the SAXS profile, we attribute it to the scattering from the partially crystalline PTMO domains of few hundred angstroms estimated from the broad WAXS peak widths of PTMO chains (inset of Fig. 1). The PTMO crystalline domains are virtually invisible to neutrons due to the very low scattering contrast, as mentioned previously. In the following, we focus on the scattering from the hard-segment aggregates.

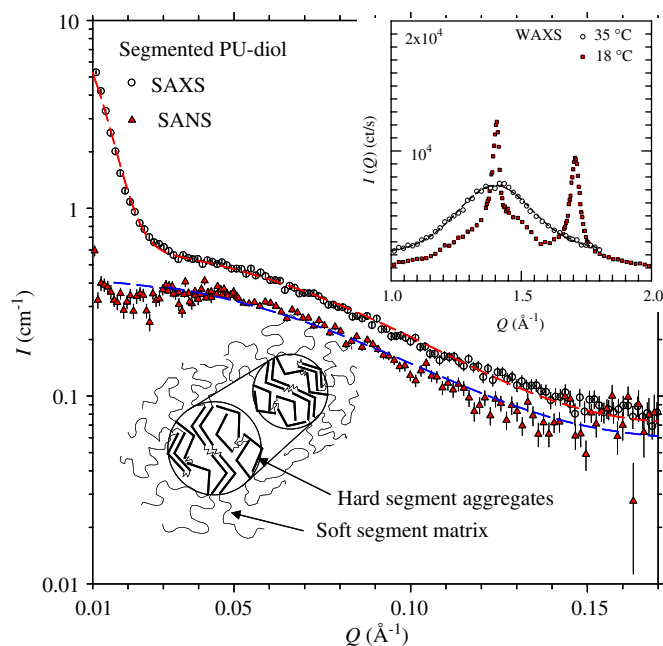


Fig. 1. The SANS and SAXS data for the segment PU film are fitted (dashed curves) using a rod-form factor with a hard-sphere structure factor. Based on the Guinier approximation, [8] we have included a term of  $I_0 \exp(-Q^2 R_g^2)$  in the fitting process to take into account the scattering contribution (mainly in the low- $Q$  region) by large PTMO crystalline domains, with a radius of gyration  $R_g \sim 140$  Å. Inset demonstrates the WAXS profiles observed for the sample at 35 and 18 °C, respectively. The cartoon illustrates a hard-segment-rich aggregate formed in the PTMO matrix.

Both the SANS and SAXS data in the region  $Q \gtrsim 0.05$  Å<sup>-1</sup> can be fitted adequately with the Kratky–Porod approximation for a rod-like shape. [8] Furthermore, distance distribution function  $p(r)$  obtained from the SANS  $I(Q)$  using the indirect Fourier transformation (IFT) for minimizing the data termination effects also indicates rod-like aggregates of a radius  $\sim 25$  Å and a length  $\sim 60$  Å. [14] Therefore, we adapt a cylinder-form factor and a hard-sphere structural factor [8,9] in our model fitting for the detailed structural information of the aggregates in the film. We integrate the SANS and SAXS data in a model-fitting algorithm, [15] which helps in reducing the fitting parameters to five, including  $r$  and  $L$  for the cylindrical form factor, and  $C_0$ ,  $N$ , and  $V_i$  for the scattering amplitude  $I_0$ . The  $S(Q)$ , depending on the volume fraction  $\eta = (C - C_0)V/N$  and an effective sphere diameter  $\sigma$  approximated using  $V_{\text{agg}} = \pi r^2 L = 4/3\pi(\sigma/2)^3$ , adds no additional parameter in the fitting algorithm. We also take into account the data-smearing effect of  $I(Q)$  due to the

beam divergence and the wavelength dispersion of the beam in the non-linear fitting process. The fitting result (dash curves in Fig. 1) demonstrates that the common rod-structure parameters  $r = 20 \pm 2$  Å,  $L = 50 \pm 5$  Å, and  $V_{\text{dry}} = 710 \pm 30$  Å<sup>3</sup> can largely satisfy both sets of data. In the fitting process,  $C_0$  and  $N$  are highly correlated, and cannot be determined with a single hard-segment concentration. Nevertheless, we present the best-fitted  $C_0 = 17.3$  wt% (90% of hard segments in the PU) and  $N = 63$ . The high  $C_0$  value for the critical aggregation concentration of the hard segments in the PTMO matrix is generally consistent with the picture given previously that hard segments of short MDI sequence can dissolve in PU elastomer well up to  $\sim 30\%$ . [5,6,9] From the volume of the aggregate  $V_{\text{agg}} = \pi r^2 L = NV_{\text{dry}} + MV_s$ , with  $V_s = 3500$  Å<sup>3</sup> for the volume of PTMO, [11] we can also deduce a PTMO association number  $M \sim 7$  for the hard-segment-rich aggregate.

## Acknowledgements

We thank Drs. L.-Y. Wang and L. Y. Chiang for providing the sample, and are grateful for the support of Drs. C. C. Han and L. P. Song.

## References

- [1] B. Chu, T. Gao, Y. Li, J. Wang, C.R. Desper, C.A. Byrne, *Macromolecules* 25 (1992) 5724.
- [2] J.T. Koberstein, T.P. Russell, *Macromolecules* 19 (1986) 714.
- [3] Y. Li, T. Gao, J. Liu, K. Linliu, C.R. Desper, B. Chu, *Macromolecules* 23 (1992) 7365.
- [4] Y.-S. Huang, Y.-N. Cheng, J.-D. Li, W.-L. Lu, H.-C. Wang, C.-H. Chao, S.-L. Chang, L.-Y. Wang, L.Y. Chiang, *Fullerene Sci. Technol.* 7 (4) (1999) 573.
- [5] L.M. Leung, J.T. Koberstein, *Macromolecules* 19 (1986) 706.
- [6] C.H.Y. Chen-Tsai, E.L. Thomas, W.J. MacKnight, N.S. Schneider, *Polymer* 27 (1986) 659.
- [7] J.T. Koberstein, A.F. Galambos, L.M. Leung, *Macromolecules* 25 (1992) 6195.
- [8] S.-H. Chen, *Ann. Rev. Phys. Chem.* 37 (1986) 351.
- [9] J.S. Higgins, H.C. Benoit, in: *Polymer and Neutron Scattering*, Clarendon Press, Oxford, 1994.
- [10] B. Cabane, R. Duplessix, T. Zemb, *J. Phys.* 46 (1985) 2161.
- [11] L.Y. Chiang, L.-Y. Wang, C.-S. Kuo, *Macromolecules* 28 (1995) 7574.
- [12] B. Jacrot, *Rep. Prog. Phys.* 39 (1976) 911.
- [13] T.P. Russell, H. Ito, G.D. Wignall, *Macromolecules* 21 (1988) 1703.
- [14] O. Glatter, *J. Appl. Crystallogr.* 21 (1988) 886.
- [15] U. Jeng, C.-S. Tsao, C.-H. Lee, T.-L. Lin, L.-Y. Wang, L.Y. Chiang, C.C. Han, *J. Phys. Chem. B* 103 (1999) 1059.